NUMERICAL SIMULATION AND MODELLING OF A TYPICAL SWIMMING POOL FOR DISINFECTION BY-PRODUCTS ASSESSMENT

CLOTEAUX Anaëlle [1], GERARDIN Fabien *, MIDOUX Noël [2]

[1] Département Ingénierie des Procédés, Institut National de Recherche et de Sécurité (INRS) – France
[2] Laboratoire de Réactions et Génie des Procédés (LRGP), Centre National de la Recherche Scientifique (CNRS) – Ecole Nationale Supérieure des Industries Chimiques (ENSIC) – France

ABSTRACT
A study was performed to investigate the use of Computational Fluid Dynamics (CFD) for determining real swimming pool hydraulic model. The main aim of this study was to provide a simple hydraulic model for optimising chlorination or for predicting the kinetic of disinfection by-products. This work consisted, on the basis of a pool flow simulation (velocity field and path lines), in comparing the simulated integral Residence Time Distribution (RTD) and the integral RTD of the model. This model was based on the association of two Constant Stirred Tank Reactors (CSTRs) with an exchange flow between them. Each CSTR was relevant to the part of the pool identified by the simulation. The simulation also allowed determination of the different parameters of the model chosen. The representation of the modelled RTD turned out to be very close to the simulated RTD highlighted the relevance of model choice pertinence for this kind of pool. This study demonstrated that it is possible to avoid the systematic use of CFD for assessing the evolution of the chemical species in the experimental pool.

Keywords	CFD, swimming pool, hydraulic model, RTD (residence time distribution), chlorination by-products

INTRODUCTION
Knowledge of the chemical reactions involved along with identification and quantification of swimming-pool water chlorination by-products have, in recent years, become major preoccupations for World Health Organization (WHO, 2006). While some scientific works available in the literature yield information about the kinetics of the chlorination of the nitrogenous compounds brought by swimmers like ammonia and urea (Jafvert and al., 1992 – Ozekin and al., 1996), most authors describe only the time evolution of the species concentrations in the pool (Li and al., 2007 – Weaver and al., 2009)

Considered as a real chemical reactor (supplied with reagent hypochlorite and nitrogenous compounds and exchanging species by its surface) including a recycling loop, pools have rarely been studied from a hydraulic aspect (Liu and al., 2006 – Stamou, 2008). Even so, the flow characterisation of the pool, by depending on its recirculation, mixing areas or its dead spaces, is a determining step for chlorination optimisation or for kinetic prediction.

Thus, for a pool with traditional geometry and operating in reversed hydraulicity, a study aimed at its hydraulic modelling is proposed in this document. This approach consists, from the pool flow simulation (velocity field and path lines) and from the Residence Time Distribution (RTD) established without a recycling loop, in building a basic hydraulic model. This model will allow more convenient prediction of the evolution of the concentration of the chemical species present in the pool. It will also enable the planning of a relevant strategy for the control of some species such as chloramines and chloroform in the pool.

MATERIAL AND METHODS

The volume and the surface area of the pool studied are 536 m^3 and 275 m^2 respectively. The pool dimensions are represented in the figure 1. The pool is fed with water via three square inlets in cross-section (0.3m x 0.3m) located on one of the vertical walls. The inlet flow-rate is equal to 5.10^{-2} $m^3.s^{-1}$. The water is collected at the pool surface by overflow channels (0.02m x 25m). This kind of pool with traditional geometry is quite common particularly in France.

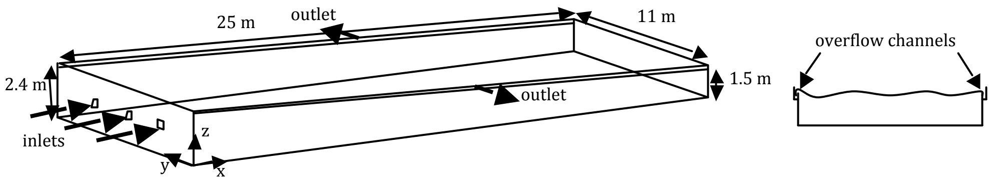

Figure 1 Pool geometry and dimensions

The flow simulation allows determination of the velocity field, the path lines in the area studied or to the RTD of the system. The simulation is performed without swimmers and only takes account of the inlet and outlet flow of the pool.

From the simulation results, a basic and a pool-equivalent hydraulic model will be proposed. This hydraulic model will be constructed by associating basic reactors whose global RTD will be compared to the RTD of pool studied.

FLOW SIMULATION

ANSYS FLUENT, a Computational Fluid Dynamics (CFD) code based on the finite volume method, was used in this study. The equations of the model are solved over each control volume, such that the relevant quantity (mass, momentum, tracer concentration, etc.) is conserved. The Upwind first order method was used to solve the differential equations governing fluid flow. Pressure and velocity are coupled by means of the SIMPLE scheme.

TURBULENCE MODEL

The inlet jet Reynolds number ($Re = {}^{\rho u d}/_{\mu}$ where u is the inlet velocity and d is the inlet hydraulic diameter) for the pool studied is equal to 55,500 but some areas present very low velocities. Therefore, the RNG $k - \varepsilon$ turbulence model was chosen. The «renormalization group» (RNG) theory provides an analytically-derived differential formula (eq. 1) for effective viscosity (μ_{eff}) that accounts for low-Reynolds-number effects (Ansys Fluent 12, 2009).

$$d\left(\frac{\sqrt{\rho k}}{\sqrt{\varepsilon\mu}}\right) = 1.72\frac{{}^{\mu_{eff}}/_{\mu}}{\sqrt{\left({}^{\mu_{eff}}/_{\mu}\right)^2 - 99}}\,d\left({}^{\mu_{eff}}/_{\mu}\right) \qquad (1)$$

Equation 1 is integrated to obtain an accurate description of the effective turbulent transport variations with the effective Reynolds number, allowing the model to better handle low-Reynold-number and near-wall flows. The coefficients for the RNG $k - \varepsilon$ model are $C_1 = 1.42$, $C_2 = 1.68$, $C_\mu = 0.0845$.

NUMERICAL GRID

The flow field simulation is carried out for a half pool, considering that the plane of equation y = 5.5m is a plane of symmetry (cf. Figure 2). A hexahedral meshing is constructed with the Gambit© software. Cells have a length of 0.5m in the *x* direction and 0.1m in the *y* direction. Their height in the *z* direction is between 0.02m and 0.1m. The meshing of the half pool is composed of 77,000 cells.

BOUNDARY CONDITIONS

- Inlet conditions: uniform inlet velocity equal to $0.185 m.s^{-1}$ in the x direction. At the inlet, the initial values of k and ε are $1.28 \times 10^{-4} m^2.s^{-2}$ and $1.13 \times 10^{-5} m^2.s^{-3}$ respectively.
- Outlet conditions: outlet pressure imposed (relative pressure of 0 bar).
- Water surface: wall with slide.
- Pool wall: walls without slide (roughness 0.5mm). The standard wall function approach was applied.

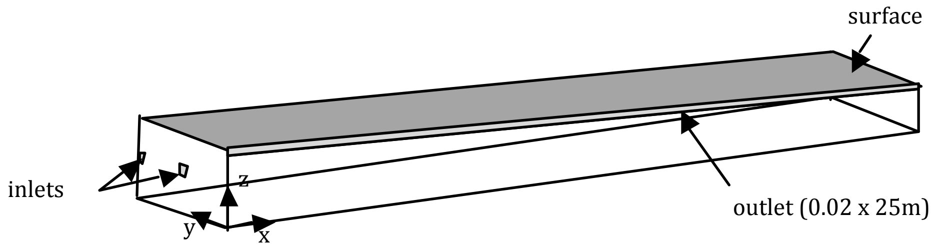

Figure 2 Geometry of the half pool

RESIDENCE TIME DISTRIBUTION

The following strategy was used to determine the Residence Time Distribution (RTD):

(1) The conservation of momentum equation and the RNG k – ε turbulence equations were solved until a steady-state solution was reached.

(2) A step impulse of an inert tracer was added to the inlet flow at a concentration c0. Using the steady-state flow solution as the initialization, the same equations were solved in transient state.

The tracer convection-diffusion equation is:

$$\frac{\partial \rho c}{\partial t} + \frac{\partial \rho U_{xi} c}{\partial x_i} = \frac{\partial}{\partial x_i}\left(\left(\frac{\mu}{Sc} + \frac{\mu_\tau}{Sc_\tau}\right)\frac{\partial c}{\partial x_i}\right) \quad (2)$$

where $Sc_\tau = 1$ is the turbulent Schmidt number for the tracer.
To obtain the integral distribution *F(t)*, the tracer concentrations *c(t)* at the outlet of the pool are divided by the inlet concentration c_0 (eq. 3).

$$F(t) = \frac{c(t)}{c_0} \quad (3)$$

The function *F(t)* represents the probability that part of the water in the pool has a residence time less than or equal t.
The RTD is deduced from *F(t)* as follow:

$$E(t) = \frac{dF}{dt} \quad (4)$$

POOL MODELING

The aim is to represent the pool by an ideal reactor or an association of ideal reactors. The main ideal reactors are the Continuous Stirred Tank Reactor (CSTR) and the Plug Flow Reactor (PFR). These reactors can be associated in series or in parallel in order to create a model of a real reactor. Short circuiting, dead zones and recycling can also be taken into account. The types of reactors and associations can be deduced from the residence time distribution.

3. RESULTS AND DISCUSSIONS

The equations governing the flow field were solved in steady-state conditions with residue convergence criteria of 10^{-3}.

In figure 3, the velocity fields in a horizontal plane located at a distance from the surface of *z*=1.2m and in a vertical plane located at *y*=5.5m are shown. The main characteristic of this flow field is the formation of two massive recirculation regions which occupy half the pool. The flow entering via the left-hand-inlet forms an anti-clockwise recirculation region and the right-hand inlet flow forms a clockwise recirculation area. Very low velocities are found in the half pool far from the inlets, coming primarily from the central jet.

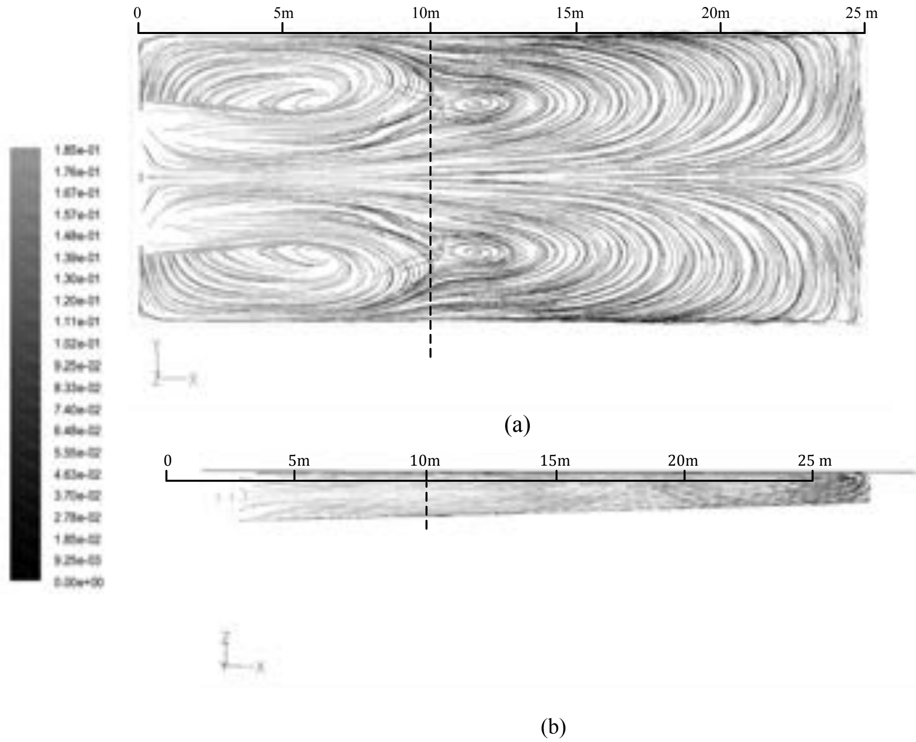

Figure 3 Path lines coloured by velocity magnitude ($m.s^{-1}$) (a) (*xy*) plane at z = 1.2m. (b) (*xz*) plane at *y* = 5.5m.

The simulation results indicate a low turbulent kinetic energy dissipation per mass unit, ε, in the order of 10^{-7} $m^2.s^{-3}$ and a global dissipation of 0.34W for the entire pool. Detailed examination of figures 3a and 3b allow us to distinguish two distinct areas in the pool. The first is located at the inlets side and is 10m long and 11m wide. The second corresponds to the weakly agitated part of the pool. It extends over the entire width of the pool and between *x* = 10m and *x* = 25m.

From these observations, an elementary hydraulic model is proposed. This model is based on the association of two CSTRs. Each CSTR is relevant to a previously identified part of the pool (cf. figure 4). An exchange flow is provided between the two reactors and each reactor owns one outlet. The outlet flows of these reactors are then collected together.

The *a* and *b* parameters enable the volume and the outlet flow rate respectively of each reactor to be balanced. The *c* parameter is related to the balancing coefficient of the flows exchange between the two compartments of the system. *a*, *b* and *c* constitute the model parameters.

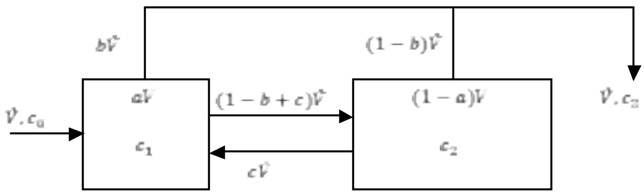

Figure 4 Scheme of the hydraulic model.

The study of the global RTD of the equivalent model consists in analytically determining the evolution of the concentration in the two compartments ci(t) for a passive scalar injected in the form of a step impulse.

Hence, for such a system, the equations governing the concentration *ci(t)* for a step impulse at $t = 0$ are:

$$aV\frac{dc_1}{dt}+(1+c)\dot{V}c_1=\dot{V}c_0U(t)+c\dot{V}c_2$$

$$(1-a)V\frac{dc_2}{dt}+(1-b+c)\dot{V}c_2=(1-b+c)\dot{V}c_1 \qquad (5)$$

$$c_2=bc_1+(1-b)c_2$$

with:

$$\lambda_1=\frac{1+c}{a}\lambda_2 \quad \lambda_2^1=\frac{1-b+c}{1-a} \qquad (6)$$

$$\tau=\frac{V}{\dot{V}} \qquad \theta=\frac{t}{\tau}$$

and:

$$C_i=\frac{c_i}{c_0} \qquad (7)$$

- τ is the global average residence time in the pool,
- $\lambda_1 = \tau/\tau_1$ where τ_1 is the average residence time in the first compartment,
- $\lambda_2 = \tau/\tau_2$ where τ_2 is the average residence time in the second compartment.

Eq. 5 + Eq. 6 + Eq. 7 →

$$\frac{dC_1}{d\theta}+\lambda_1 c_1=\frac{1}{a}U(\theta)+\left(\lambda_1-\frac{1}{a}\right)c_2 \qquad (8)$$

$$\frac{dC_2}{d\theta}+\lambda_2 c_2=\lambda_2 c_1$$

$$C_2=bC_1+(1-b)C_2$$

This coupled system is solved by elimination or by Laplace transformation. If the Laplace variable is *s* and:

$$\bar{C}(s)=L[c(\theta)]$$

$$\bar{C}_2 = \frac{\lambda_2}{as\left[s^2 + (\lambda_1 + \lambda_2)s + \frac{\lambda_2}{a}\right]}$$

$$\bar{C}_2 = \frac{\lambda_2}{s + \lambda_0}\bar{C}_1 \quad (9)$$

$$\bar{C}_2 = b\bar{C}_1 + (1 - b)\bar{C}_2$$

and:

$$r1r2 = \frac{1}{2}[(\lambda_1 + \lambda_2 \pm \sqrt{\Delta}]$$

$$\Delta = (\lambda_1 + \lambda_2)^2 - \frac{4\lambda_2}{a}$$

$$C_1(\theta) = 1 + \frac{1}{a(r_1 - r_2)}\left[\left(1 + \frac{\lambda_2}{r_1}\right)e^{r_1\theta} - \left(1 + \frac{\lambda_2}{r_2}\right)e^{r_2\theta}\right] \quad (10)$$

$$F(\theta) = C_2(\theta) = bC_1(\theta) + (1 - b)C_2(\theta)$$

$$E(\theta) = \frac{dF(\theta)}{d\theta} = \frac{1}{a(r_1 - r_2)}[(br_1 + \lambda_2)e^{r_1\theta} - (br_2 + \lambda_2)e^{r_2\theta}]$$

The average of the RTD $E(\theta)$ is equal to 1 and the variance, which characterises the dispersion around the average, is given by:

$$\sigma^2 = 2a\left[1 + \frac{\lambda_1 - 1}{\lambda_2}\right] - 1 \quad (11)$$

The variance of a CSTR is equal to 1. The variance calculation enables the difference between the RTD of the proposed model and that of a CSTR to be evaluated.

For instance, the figure 5 represents the integral RTD of the entire system and those of each hydraulic model compartment. In this case, the a, b and c coefficients are 0.5, 0.75 and 0.2 respectively. Thus, the variance is close to unity (σ^2=1.56) and the global RTD of the proposed system would appear to be close to CSTR RTD. Moreover, the table 1 gives more information on the influence of the parameters *b* and *c* regarding the difference between the model and a CSTR.

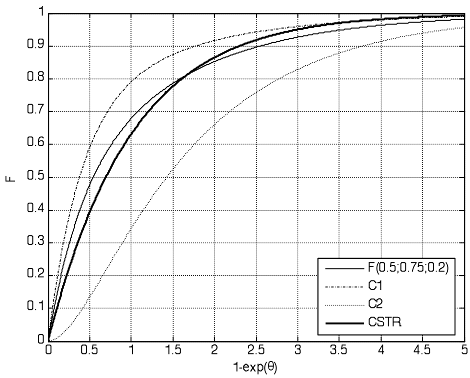

Figure 5 Distributions $F(\theta)$ and adimensional concentrations $C_1(\theta)$ and $C_2(\theta)$ for conditions (0.5;0.75;0.2) compared to that of a CSTR.

Table 1 Variance of RTD for different models

	« Average » case	b influence			c influence		
a	0.5	0.5	0.5	0.5	0.5	0.5	0.5
b	0.75	0.25	0.5	0.75	0.25	0.25	0.25
c	0.2	0	0	0	0.2	0.5	1
λ_1	2.4	2	2	2	2.4	3	4
λ_2	0.9	1.5	1	0.5	1.9	2.5	3.5
σ^2	1.56	0.67	1	2	0.74	0.8	0.86

Figures 6 and 7 illustrate the respective influence of the *b* and *c* parameters on the global RTD of the model for an impulse step and with $a = 0.5$.

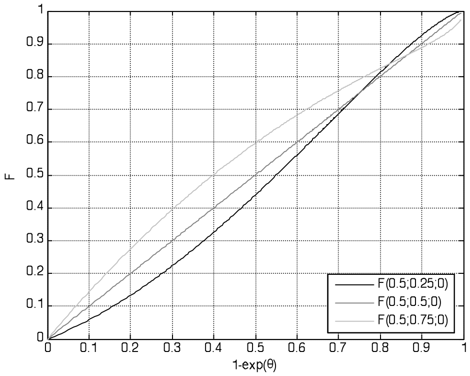

Figure 6 Influence of the b parameter on the distributions $F(\theta)$ for two compartments of the same volume and without exchange flow.

Figure 6 shows the influence of the distribution of the outflows. The representation of $F(\theta)$ in function of the CSTR distribution allows the model distribution to be compared with a CSTR, fitted by the diagonal. It would appear that the *b* coefficient of the model has a significant influence and may explain the difference between the real system RTD and the CSTR RTD.

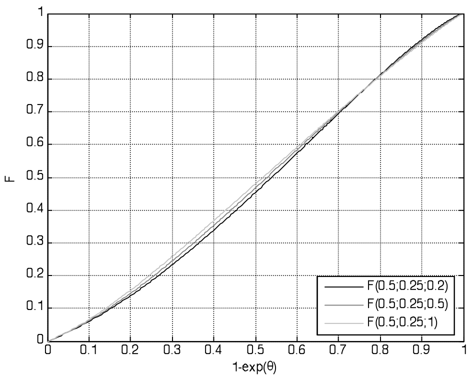

Figure 7 Influence of the c parameter on the distributions $F(\theta)$ with average *a* and *b* parameters.

Examination of the figure 7 allows to be concluded that the exchange flow between the two areas of the pool, characterised by the *c* parameter, has no significant influence on the global RTD of the pool studied.

In the case of the experimental pool, the flow simulation shows that the limit between the «agitated» area and the «quite stagnant» area is located 10m from the inlets. The volumes of the first and second compartment are 246.6 m^3 and 289.4 m^3 respectively. The *a* coefficient, wich represents the ratio of the agitated area volume to the entire pool volume, is equal to 0.46.

The *b* coefficient of the model corresponds to the fraction of the total flow-rate and represents the outlet flowrate of the first part of the pool. This outlet flow rate is calculated by integrating the velocity (U_y) in function of x over the 10 first meters of the overflow channels. The water is collected by the overflow channels located on each lateral wall of the pool with a film thickness of 0.02m. The section crossed by water at each overflow channels in the first compartment is thus 10 x 0.02 = 0.2m^2. Moreover, the velocity $U_y(x)$ is obtained by the simulation (cf. figure 8). The outlet flow rate of the first compartment is equal to 9 x $10^{-3}m^3.s^{-1}$, i.e. 35% of the inlet flow-rate (b = 0.35). The outlet flow rate of the second compartment is 4.1 x $10^{-2}m^3.s^{-1}$.

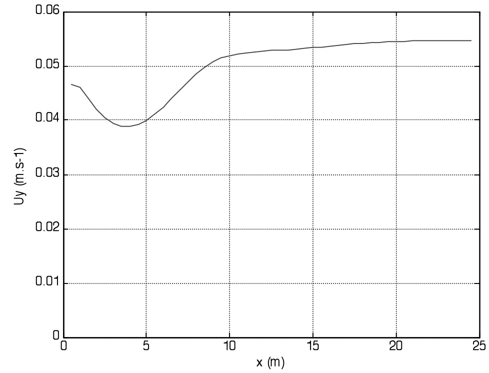

Figure 8 Velocity U_y profile at one of the two pool overflow channels.

Finally, the last model parameter c defining the recirculation rate between the «agitated» area and the «quite stagnant» area is determined from the simulation results; more precisely, by integrating the U_x component in the (*yz*) plane located at x = 10m (cf. figure 9).

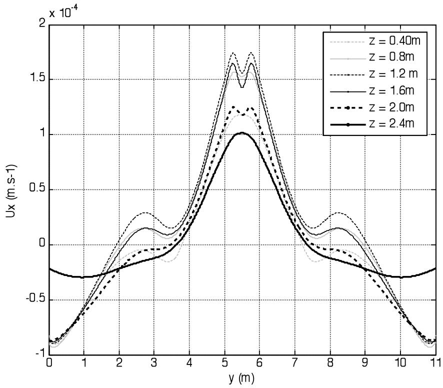

Figure 9 U_X velocity profile in the plane X = 10m for different heights Z (water surface at Z=2.4m).

The net exchange flow between the two compartments, defined from the material balance presented in figure 4, is:

$$(1-b-c)\dot{V} = 9.2\times10^{-2} m^2.s^{-1}$$

that is

$$c\dot{V} = 6.0\times10^{-2} m^2.s^{-1}$$

The c parameter is 1.22 and the b parameter value was confirmed to be 0.35.

Determining a, b and c parameters of the hydraulic model proposed for the experimental pool now enables a representation of the global RTD of the model. This RTD is calculated from the equations (10) that characterise pool dynamics studied for an impulse step perturbation.

The λ_1 and λ_2 parameters of the pool studied are therefore equal to 4.83 and 3.39 respectively. The variance (σ^2) is around 0.94. Figure 10 illustrates the simulated and modelled integral RTD for the pool studied. Examining these representations, it would appear that the two RTDs are very close, which confirms the relevance of the hydraulic model proposed.

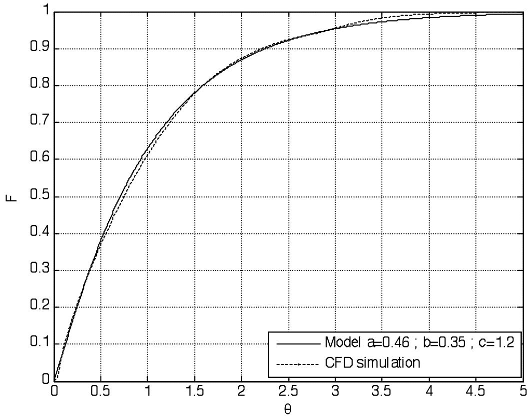

Figure 10 Representation of the simulated and modelled integral RTD.

CONCLUSION

CFD simulation allows characterisation of the water flow in a wide range of pools with different geometries and operating modes. The velocity field and the path lines simulated in the pool volume have revealed that most of the feed jet is dissipated in the first 10 meters of the pool and that this involves relatively intense water recirculation in this part of the pool. Detailed examination of the simulation results reveals that the pool is composed of an «agitated» and a «stagnant» areas.

From these observations, it has been possible to build a simplified hydraulic model of the experimental pool. This model is based on representing the two parts of the pool as CSTR with their own outlet and an exchange flow between them.

The simulation is capable of determining the different parameters of the model chosen. The representation of the modelled RTD turns out to be very close to the simulated RTD, which shows the relevance of the choice of model.

Lastly, this works has confirmed that it is possible to represent a complicated real flow as a simplified model. This model, suitable for pools with comparable operating and geometric configurations, has proved to be especially convenient for kinetics applications, in particular for predicting the concentration of the chemical species present in the pool. It is possible, without too much difficulty, to adapt this approach to other pool configurations by applying an appropriate modelling scheme.

REFERENCES

Ansys Fluent 12, 2009. Theory guide. chapter 4 Turbulence

Jafvert, CT and Valentine, RL, 1992. Reaction scheme for the chlorination of ammoniacal water. *Environmental Science & Technology*, 26: 577-586

Li, J and Blatchley III, ER, 2007. Volatile disinfection byproduct formation resulting from chlorination of organic-nitrogen precursors in swimming pools. *Environmental Science & Technology*, 41, (19): 6732–6739

Liu, Y and Ducoste, J, 2006. Numerical simulation of chloramines in turbulent flow using a multi-fluid micromixing model. *Environmental Modelling and Software*, 21, (8): 1198-1213

Ozekin, K, Valentine, RL and Vikesland, PJ, 1996. Modeling the decomposition of disinfecting residuals of chloramines, in Minear, R and Amy, G, Water disinfection and natural organic matter: Characterization and Control, ACS Books, Washington D.C, pp. 115-125

Stamou, AI, 2008. Improving the hydraulic efficiency of water process tanks using CFD models. *Chemical Engineering and Processing*, 47: 1179–1189

Weaver, WA, Li, J, Wen, Y, Johnston, J, Blatchley, MR and Blatchley III, ER, 2009. Volatile disinfection by-product analysis from chlorinated indoor swimming pools. *Water Research*, 43: 3308-3318

World Health Organization (WHO), 2006. Guidelines for the safe recreationnal water environments. *Swimming pools and similar environments*, Vol. 2

NOMENCLATURE

cj	tracer molarity in the j compartment, [$mol.m^{-3}$]
d	inlet hydraulic diameter, [m]
D	molecular diffusivity coefficient, [$s.m^{-2}$]
D_T	turbulent diffusivity coefficient, [$s.m^{-2}$]
k	turbulent kinetic energy per unit mass, [$m^2.s^{-2}$]
t	time, [s]
u	inlet velocity, [$m.s^{-1}$]
U_i	velocity in the i direction, [$m.s^{-1}$]
V	volume, [m^3]
$\dot{V}$	volume flow rate, [$m^3.s^{-1}$]
x_i	direction i ($x_1 = x$, $x_2 = y$, $x_3 = z$), [m]

Symbols

ε	turbulent kinetic energy dissipation rate per mass unit, [$m^2.s^{-3}$]
μ	liquid molecular viscosity, [Pa.s]
$\mu_{\varepsilon\phi\phi}$	$= \mu + \mu_T$, liquid effective viscosity, [Pa.s]
μ_T	liquid turbulent viscosity, [Pa.s]
ρ	water density, [$kg.m^{-3}$]
ν	liquid kinetic viscosity, [$m^2.s^{-1}$]
τ	$=V/\dot{V}$, pool average residence time, [s]

Indices

i	direction (i = 1, 2 or 3)
j	compartment (j = 1 or 2)
0	pool inlet

Adimensional numbers

a	part of volume of the first compartment
b	part of the total flow-rate leaving the first compartment
c	part of the exchange flow-rate between the two compartments
C_1	constant of the k-ε model
C_2	constant of the k-ε model
C_m	constant of the k-ε model
E	residence time distribution
F	integral residence time distribution
Re	$\rho ud/\mu$,inlet jet Reynolds number
θ	$= t/\tau$, adimensional time
λ_1	$= (1+c)/a$, ratio of the average residence time of the first compartment at the global average residence time
λ_2	$= (1-b+c)/(1-a)$, ratio of the average residence time of the second compartment at the global average residence time
σ''	variance of the residence time distribution
Sc	$=\mu/\rho D$,laminar Schmidt number for the tracer
Sc_T	$=\mu_T/\rho D_T$,turbulent Schmidt number for the tracer
U	unit step